euronoise

Ultrasonic diffraction grating spectroscopy: particle size measurements and investigation of the inertial model for attenuation

Margaret Greenwood

Pacific Northwest National Laboratory, P. O. Box 999, Mailstop K5-26, Richland, Wa, WA 99352, USA
margaret.greenwood@pnl.gov

Using the technique of ultrasonic diffraction grating spectroscopy (UDGS), data have been obtained for slurries of polystyrene spheres in water for nine particle sizes, ranging from 45 μm to 467 μm, and for concentrations up to a volume fraction of 0.20. The basic data are the FFT amplitude as a function of frequency and the value of the critical frequency. The velocity of sound in the slurry is obtained from the critical frequency. Data have been obtained for the transmitted spectral orders m = 1 and m = 2. The results of experiments over this large range of particle diameters show different behaviors for the larger diameter particles than for the smaller ones. In this paper the experimental setup and data are presented, including a discussion of trends in the data. At the Conference, the evanescent wave production and the calculation of the attenuation will be presented. The development of UDGS can lead to an on-line instrument or a laboratory instrument to measure particle size and concentration.

1 Introduction

An in-depth study of ultrasonic diffraction grating spectroscopy for the measurement of particle size is presented here. Another objective is to calculate the attenuation coefficient and compare the results with theoretical models. This subject was introduced in 2005 [1], where experimental data and the underlying physics and mathematics were presented. Earlier research is discussed in Ref. 2–4.

A schematic diagram of the experimental setup and data acquisition system is shown in Fig. 1. The ultrasonic beam produced by the send transducer A strikes the grating and some fraction of the ultrasound is reflected to the receive transducer B. The front of the grating is in contact with the slurry. A magnetic stirrer below the cup keeps the suspension uniform. Transmitted beams with spectral orders m = 0, 1, and 2 are produced in the slurry. The m = 0 beam is produced at an angle due to refraction, based upon Snell's law; its angle is fixed and independent of the frequency. However, for m = 1 (m = 2) the angle of the transmitted beam with the normal to the grating surface increases as the frequency of the beam decreases. The frequency at which it reaches 90° is called the critical frequency and the transmitted wave becomes an evanescent wave. An evanescent wave travels parallel to the grating surface, but its amplitude decreases exponentially with the distance from the grating surface. The critical frequencies are nominally 3.5 MHz for m = 1 and 7.0 MHz for m = 2, for a grating spacing of 483 micrometers. Slightly below the critical frequency, a transmitted beam can no longer exist in the liquid or slurry. Its energy is transferred to other beams, such as that reflected to receive transducer B, where the signal shows a peak at the critical frequency. For slurries, the evanescent wave interacts with the particles of the slurry and its amplitude is reduced. The peak amplitude is found to depend on the particle size and concentration of the slurry and, thus, provides a means for determining the particle size. The measurement of the critical frequency at which the peak occurs leads to a determination of the velocity of sound in the liquid or slurry [1].

In the current research, data have been obtained for spectral orders m = 1 and m = 2 for slurries of nine diameters of polystyrene spheres—45 μm to 467 μm, with concentrations ranging up to a volume fraction of 0.20. The data are analyzed using the *area* under the peak. The attenuation coefficient can be obtained by comparing the results with water with that for a given slurry concentration. When the energy of the evanescent wave in water is transformed to energy of other beams, part of this energy from this transition is observed by the receive transducer. Similarly, the evanescent wave in the slurry has a reduced amplitude due to interaction with particles, but then its remaining energy is likewise transformed into other beams and observed by the receive transducer. We shall assume that the fraction of the energy for water monitored by the receive transducer is the same as that for the slurry. Thus, energy conservation yields the following:

$$\begin{pmatrix}\text{Energy Content}\\ \text{of Evan. Wave}\\ \text{for Water}\end{pmatrix}=\begin{pmatrix}\text{Energy Content}\\ \text{of Evan. Water}\\ \text{for Slurry}\end{pmatrix}+\begin{pmatrix}\text{Energy Dissipated}\\ \text{During}\\ \text{Attenuation}\end{pmatrix}$$

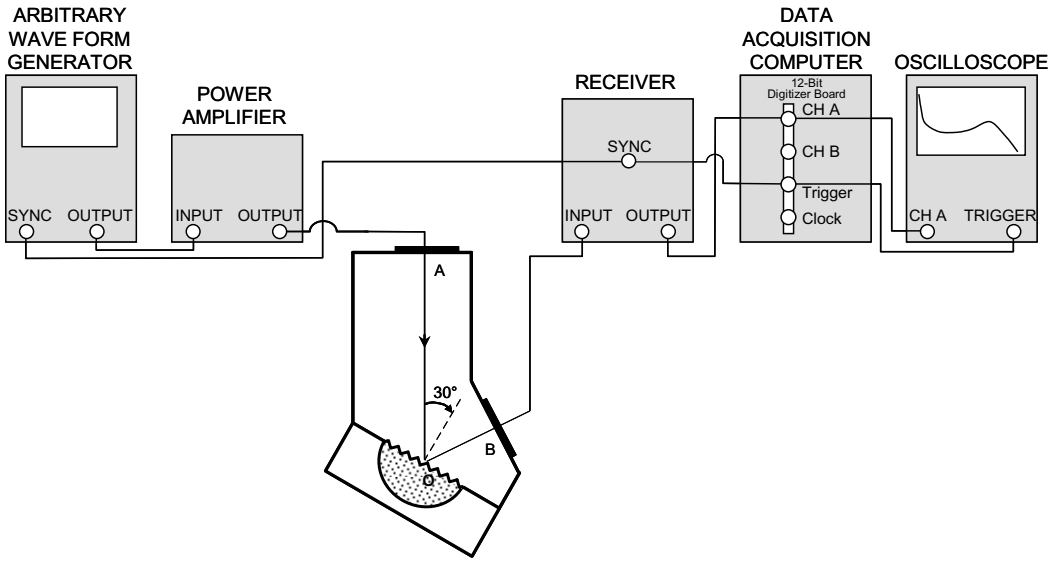

Fig. 1. Experimental setup and data acquisition system.

The resulting calculation leads to the attenuation coefficient.

The results of experiments over this large range of particle diameters show different behaviors for the larger diameter particles than for the smaller ones. These results will be used to explore the types of interactions that are responsible for this difference in behavior.

2 Data acquisition

The grating unit in Fig. 1 was fabricated by electrical discharge machining. The basic design was for a symmetric triangular groove with an included angle of 110° and a grating spacing of 482.6 micrometers. However, as fabricated, the groove had a shallower, curved cross section as shown in Fig. 2. Knowledge of the shape of the groove is important because the shape affects the values of transmission and reflection coefficients for various spectral orders, which is a very well-known effect for optical diffraction gratings [5].

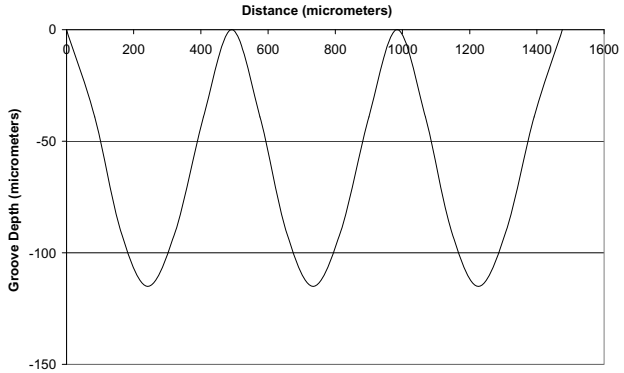

Fig. 2. Cross-section of grating surface for aluminium grating shown in Fig. 1.

Polystyrene spheres having diameters between 100 µm and 500 µm were sieved to obtain the following smaller-size ranges and were the same as those in Ref. [1]: (1) 180–250 µm, (2) 250–300 µm, (3) 300–425 µm, and (4) 425–500 µm. Additional samples were obtained for the following average particle sizes with the standard deviation of the mean: (5) 45 ± 7 µm, (6) 71 ± 11 µm, (7) 98 ± 16 µm, (8) 134 ± 21 µm, and (9) 222 ± 27 µm.

The chirp signal produced by the arbitrary waveform generator is amplified by the power amplifier and sent to transducer A in Fig. 1. The amplified signal from receive transducer B is sent to a 12-bit, 100-MHz digitizer board in the data acquisition computer, where the digitized signal is analyzed on-line and in real time using MATLAB® to obtain the fast Fourier transform (FFT) of the received chirp signal. The on-line analysis of the signal includes calculation of the FFT, averaging, and error analysis.

The objective of the chirp signal is to obtain data for the m = 1 critical frequency at 3.5 MHz and the m = 2 critical frequency at 7.0 MHz. The chirp signal is given by $e(t) \sin(2\pi f(t)\, t)$, where the frequency f(t) is 1.5 MHz initially and is 5.0 MHz at 36 microseconds, and varies linearly and continuously over this range of frequencies. The basic chirp signal is multiplied by the envelope e(t) to produce the (total) chirp signal shown in Fig. 3(a), where the actual frequencies have been reduced by a factor of 10 for the sake of illustration. From the known transducer response as a function of frequency, the chirp envelope was designed to have a strong amplification at 3.5 MHz and 7 MHz, while reducing a large response at about 6 MHz that is not of interest. The FFT of the chirp signal is shown in Fig. 3(b).

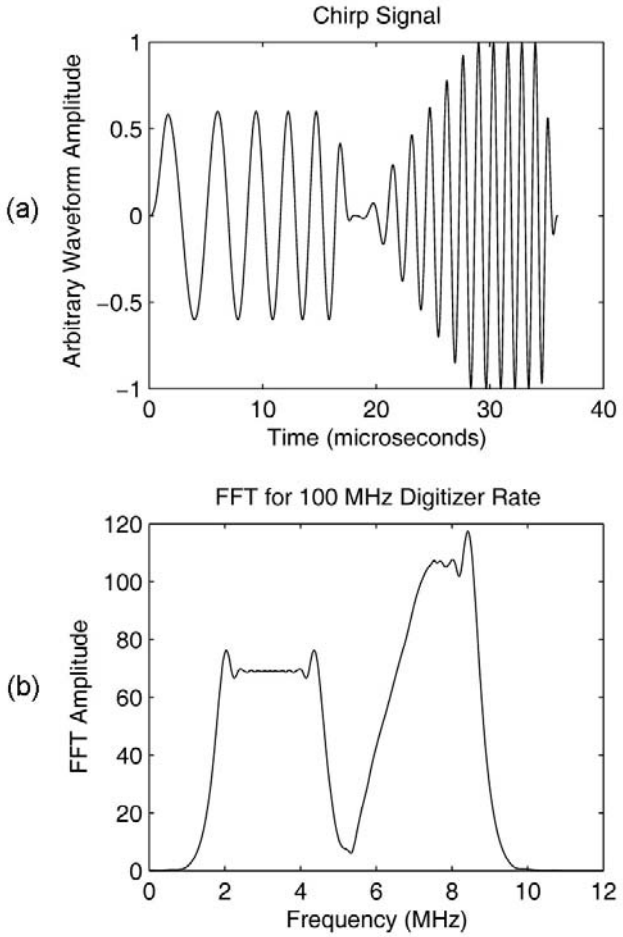

Fig. 3. Illustration of chirp signal used for the aluminium grating. (a) Chirp signal (one complete chirp) with frequency reduced by factor of 10 for illustration. (b) FFT of chirp signal.

The signal from the receive transducer B must be modified to take into account the transducer response and the chirp signal shape. Because an evanescent wave is not produced when the grating surface is in air, that signal can be used to provide the transducer response in the region of the critical frequencies for liquids and slurries. The transducer response for air (dashed line, right vertical axis) is shown in Fig. 4(a), which is obtained by dividing the average FFT amplitude for air at each frequency by the FFT amplitude at one specified value of the frequency. In this case, the frequency was chosen to be 2.905 MHz, where the FFT amplitude is 185.8 volts, so that the transducer response is 1.0 at this frequency. The average FFT amplitude for water is also shown in Fig. 4(a) (solid line, left vertical axis). In order to eliminate the transducer response, the average FFT amplitude for water is divided by the transducer response at each frequency; the result is shown in Fig. 4(b). In the data acquisition MATLAB® code, the area under the peak is calculated and the frequencies at which the maxima occur are also recorded as the critical

frequency for each peak. The latter leads to a measurement of the velocity of sound in the liquid.

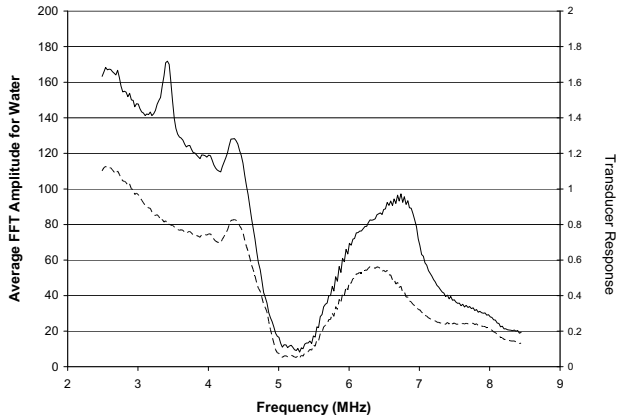

(a)

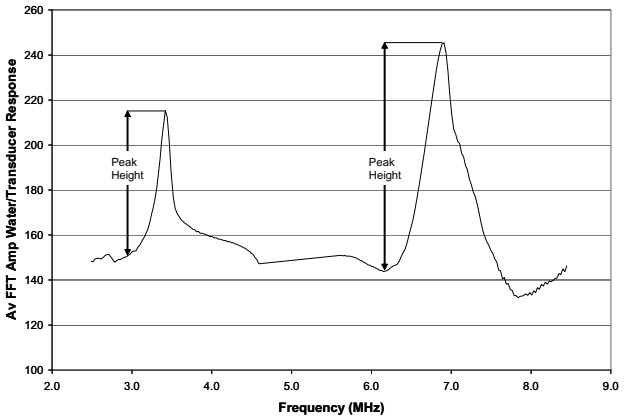

(b)

Fig. 4. Signals from the receive transducer for air and water. (a) Average FFT amplitude for water (solid line, left scale) and transducer response for air (dashed line, right scale). (b) Average FFT amplitude for water divided by the transducer response.

The peak for m = 1 at the critical frequency of about 3.5 MHz is clearly visible, as is that for m = 2 at approximately 7.0 MHz in Fig. 4. Also visible is another peak in Fig. 4(a) in the region of 5 MHz for both air and water. In addition to the m = 0 longitudinal wave reflected (diffracted) to the receive transducer, there are other spectral orders of reflected longitudinal and shear waves produced by the grating and traveling in the aluminum at an angle. In this case, when the angle for the m = -1 shear wave, traveling in aluminum, reaches -90° at its critical frequency, it becomes evanescent. At a slightly smaller frequency, the energy is shared with all other rays, including that observed by the receive transducer. The critical frequency is calculated to be 5.2 MHz. A straight line is shown in this region in Fig. 4(b), because the transducer response is not known there.

During the data acquisition, the data for air was obtained first and the transducer response was subsequently used for the data for water and slurries. Typically, a dataset consisted of 50 runs. In what follows, the data and averaging procedure used during each run is described first and then the averaging of the 50 runs is considered.

The time of flight between the two transducers is 22 microseconds and the chirp signal is 36 microseconds long. A MATLAB® code controls the digitizer card and uses commands and software from the digitizer vendor. The digitizer contains 1 MByte of memory, which is sufficient to capture 100 time signals (maximum number permitted) 58 microseconds long. The analysis of the 100 time signals is as follows: (1) The FFT is obtained for each of the 100 time signals in the region of the chirp signal. The number of points is restricted to a power of 2, 4096 in this case, to reduce the FFT calculation time. Because the digitizer rate is 100 Megasamples per second, the frequency increment is given by 1/(4096 × 0.01 microseconds), or 0.0244 MHz. (2) The 100 FFT spectra are averaged at each frequency and the standard deviation about the average is obtained. If the grating is in air, the next step is 3a: (3a) Obtain the transducer response, as has been discussed above, and use propagation of errors to determine the error at each frequency. Otherwise, the next step is 3b: (3b) Obtain the Normalized FFT Amplitude by dividing the average FFT spectrum by the transducer response, propagating the errors as in (3a). (4) The area under curve of the FFT amplitude, shown between the limits, was obtained and the background area, beneath a line drawn between the limits, was subtracted. The average of the resulting area and the standard deviation were obtained for the 50 runs. This area represents the average pressure and its standard deviation. (5) A similar procedure was carried out for the square of the FFT amplitude, because this quantity is proportional to the intensity of the wave. (6) The critical frequency f_{CR} is determined from the frequency at which the maximum FFT amplitude occurs. During each run, the critical frequency value did not vary and so the standard deviation was not obtained. In summary, the results include the FFT amplitude spectra and the critical frequency f_{CR}.

3 Discussion

Data have been obtained for polystyrene spheres in water with the following particle diameters: 45, 71, 98, 134, 215, 222, 275, 363, and 467 μm. The bottom panel of Fig. 5 shows the FFT amplitude for the peak of order m = 1 obtained for 15 concentrations, expressed in volume percentage, for polystyrene spheres having a diameter of 134 μm; the middle panel, for 275 μm; and the top panel, for 467 μm. The data for the slurry of 275 μm particles shows the greatest decrease in amplitude as the concentration increases. This decrease, of course, is an indication of the ultrasonic attenuation for that particle size. The attenuation for a slurry of 134 μm spheres in water is very small. The attenuation for a slurry of 467 μm is not as large as that for 275 μm. Similar data for other particle sizes, although not presented here, show a definite trend and are divided into two groups. For m = 1 for the larger size particles, the data show the following trend:

$$\alpha(215) > \alpha(275) > \alpha(363) > \alpha(467)$$

That is, the attenuation for a given volume percentage increases as the particle size decreases. However, for m = 1 for the smaller size particles, the trend is in the opposite direction:

$$\alpha(134) > \alpha(98) > \alpha(71) > \alpha(45)$$

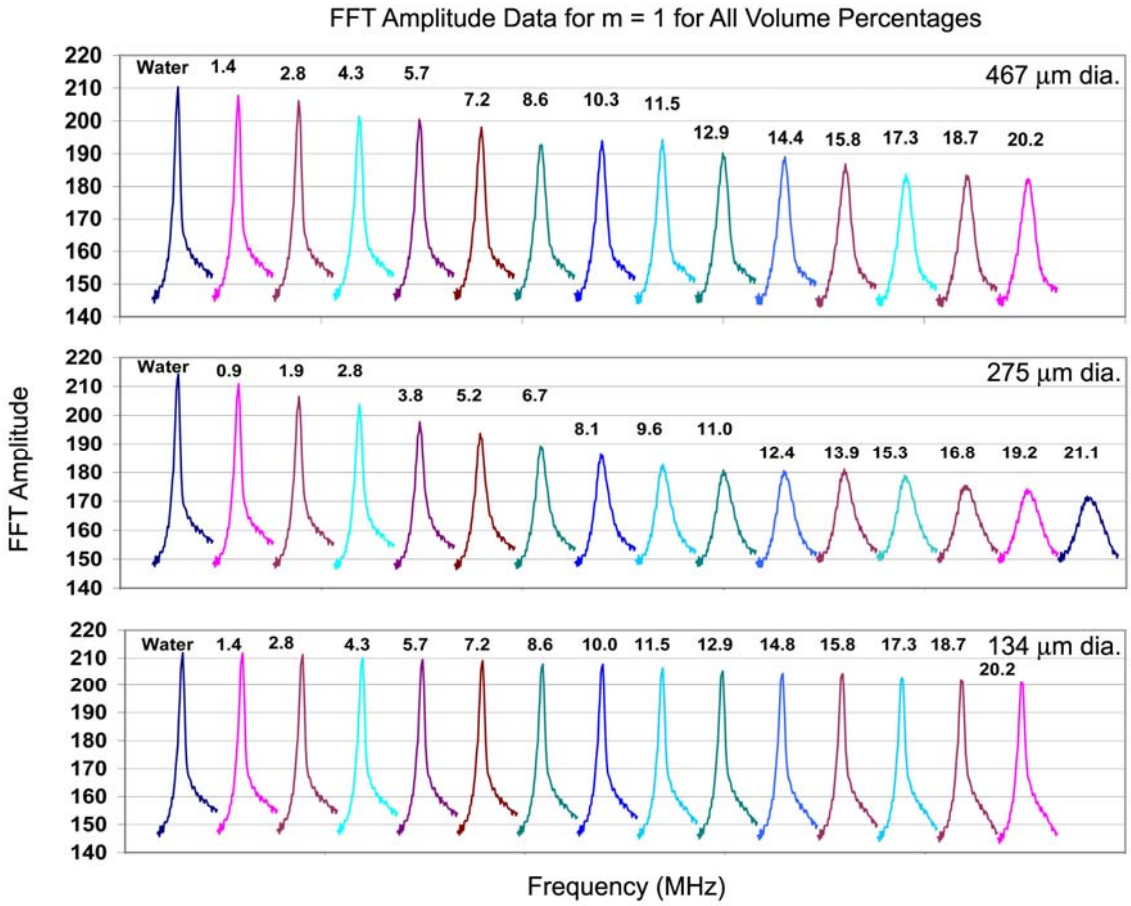

Fig 5. The FFT amplitude for water and for concentrations of polystyrene spheres in water are plotted sequentially. The particle diameter is shown in the upper right hand corner of each panel and the volume percentage is indicated above each peak. For m = 1 the frequency along the horizontal axis ranges from 2.8 MHz to 4.3 MHz.

In this group, the attenuation increases as the particle size increases.

The data for m = 2 shows similar trends, but the particle sizes in the two groups are different. Fig. 6 shows the same distributions as Fig. 5. For the larger size particles, the data show the following trend:

$$\alpha(98) > \alpha(134) > \alpha(215) > \alpha(275) > \alpha(363) > \alpha(467)$$

For m = 2 for slurries of 45 µm and 71 µm have similar values for the attenuation.

The interpretation of these results will be presented at the Conference and in a future publication.

Acknowledgments

The author wishes to thank Bruce Watson for his diligence in taking the experimental measurements. This research was supported by the Environmental Management Science Program of the Office of Science, U.S. Department of Energy (DOE). Pacific Northwest National Laboratory is operated for the DOE by Battelle Memorial Institute under Contract No. DE-AC05-76RL01830.

References

[1] Greenwood MS and S Ahmed. 2006. "Ultrasonic diffraction grating spectroscopy and the measurement of particle size." *Ultrasonics* 44:e1385-e1939.

[2] Greenwood MS, A Brodsky, L Burgess and LJ Bond. 2002. "Using ultrasonic diffraction spectroscopy to characterize fluid and slurries." In *Rev. Progr. Quant. Nondestr. Eval. (QNDE)*, 22B, pp. 1637-1643.

[3] Greenwood MS, A Brodsky, L Burgess and LJ Bond. 2006. "Investigating Ultrasonic Diffraction Grating Spectroscopy and Reflection Techniques for Characterizing Slurry Properties." In *Nuclear Waste Management: Accomplishments of the Environmental Management Science Program, Series 943*, pp. 100-132. eds: PW Wang and T Zachry. American Chemical Society.

[4] Greenwood MS, A Brodsky, L Burgess, LJ Bond and M Hamad. 2004. "Ultrasonic diffraction grating spectroscopy and characterization of fluids and slurries." *Ultrasonics* **42**:531-536.

[5] Palmer C. 2000. *Diffraction Grating Handbook*. 4th ed. Richardson Grating Laboratory.

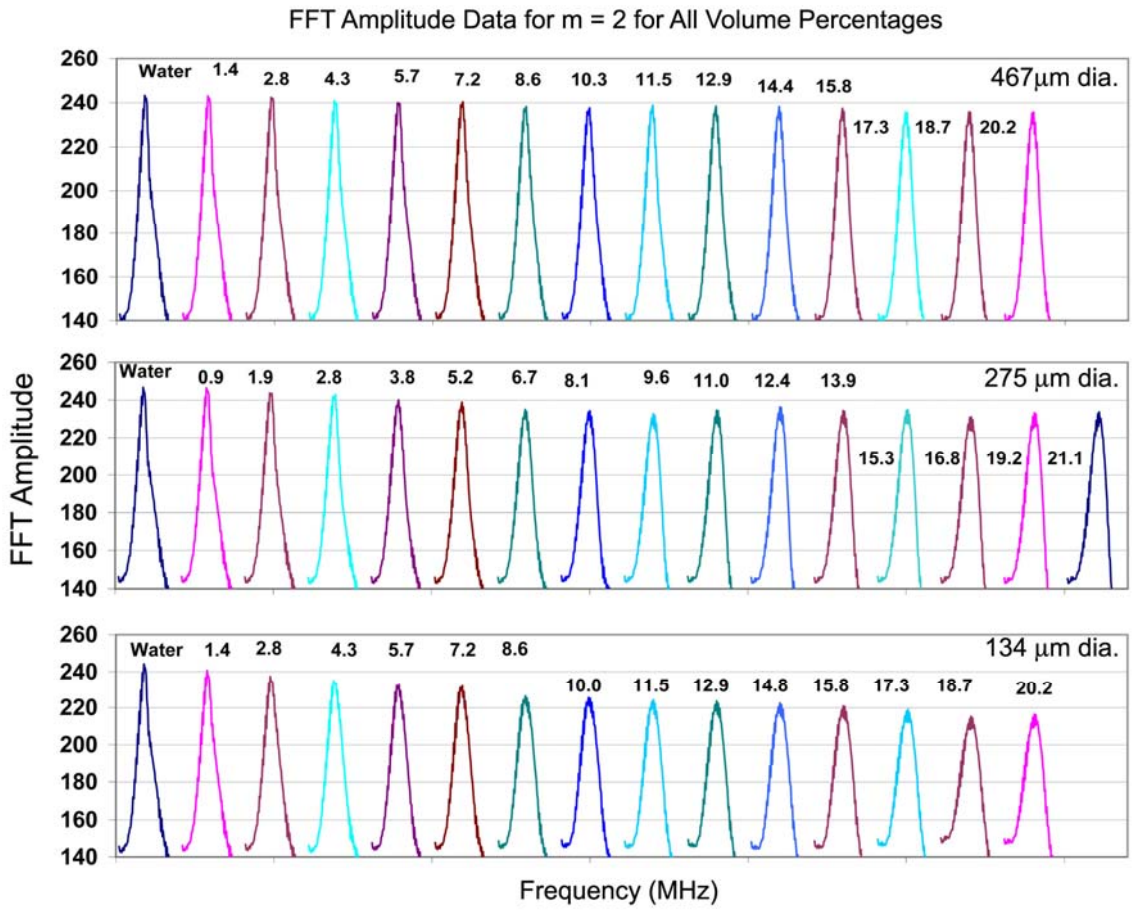

Fig. 6. The FFT amplitude for water and for concentrations of polystyrene spheres in water are plotted sequentially. The particle diameter is shown in the upper right hand corner of each panel and the volume percentage is indicated above each peak. For m = 2 the frequency along the horizontal axis ranges from 6.1 MHz to 8.0 MHz.